22 March 1996

CHEMICAL PHYSICS LETTERS

ELSEVIER

Chemical Physics Letters 251 (1996) 252-258

Covariance matrix mass spectral maps of polar dissociation channels in CF_4

L. Mi, C.R. Sporleder, R.A. Bonham

Department of Chemistry, Indiana University, Bloomington, IN 47405, USA

Received 8 August 1995

Abstract

Covariance matrix mass spectra of positive and negative ions ejected by polar dissociating states excited by electron impact on CF_4 are reported for impact energies from 18.7 to 43.7 eV. This is the first example of covariance matrix mass spectral maps of polar dissociation. Evidence for the reaction products $CF_3^+ + F^-$, $CF_2^+ + F^- + F$, $CF^+ + F^- + p$, and $F^+ + F^- + p$, where p stands for neutral species, were found. The ion translational energies are cold relative to those observed for positive ion–positive ion dissociation channels. The $CF_2^+ + F^-$ channel was observed to be the weakest and the only negative ion observed is F^-. Absolute cross section values are estimated.

Only rarely have polar dissociation (ion pair production) processes been explored by electron impact excited mass spectroscopy [1,2] and only in the former study was a coincidence experiment between positive and negative ions carried out. In addition, recent studies using photons have been reported [3,4]. In Ref. [3] the total F^- yield for CF_4 as a function of photon energy was measured. In Ref. [4] the arrival time difference between negative and positive ion time of flights was recorded for N_2O. We wish to report the first covariance matrix observations of mass spectral maps (the pulsed electron source analog to photon PEPIPICO experiments) for the negative-ion versus positive-ion mass spectrum utilizing electrons as the excitation source. The map was obtained by use of mono energetic ($\pm$ 0.6 eV) electron pulses with impact energies ranging from 18.7 to 43.7 eV impinging on an effusive gas jet of CF_4 target molecules. Three covariance matrix mass spectral maps are shown in Figs. 1a–1c. The mass spectrum shown at the top of Fig. 1a for 43.7 eV electrons impacting CF_4 is called the positive ion singles time-of-flight (TOF) spectrum and is the result of tabulating all experiments in which only a single positive ion is detected. The horizontal scale is the ion time-of-flight in nanoseconds (ns). The bottom map in Fig. 1a is the positive ion–positive ion covariance spectral map for 43.7 eV electrons impacting on CF_4 with the flight time of the first ion detected recorded on the horizontal axis in ns. The flight time of the second ion (slowest) is plotted on the vertical axis. For this same impact energy, the flight time covariance mass spectrum between positive and negative ions, produced in experiments in which only one ion of each charge state is observed, is shown in Fig. 1b. The negative ion singles spectrum (all experiments in which only one negative ion is detected) is shown at the top. The data in Figs. 1a and 1b were collected simultaneously. Note that this spectrum is completely dominated by false negative ion peaks caused by back accelerated secondary electrons produced by positive ions striking grids and detector surfaces. In Fig. 1c the same polar dissociation map and singles spectrum are

Elsevier Science B.V.
PII S0009-2614(96)00077-2

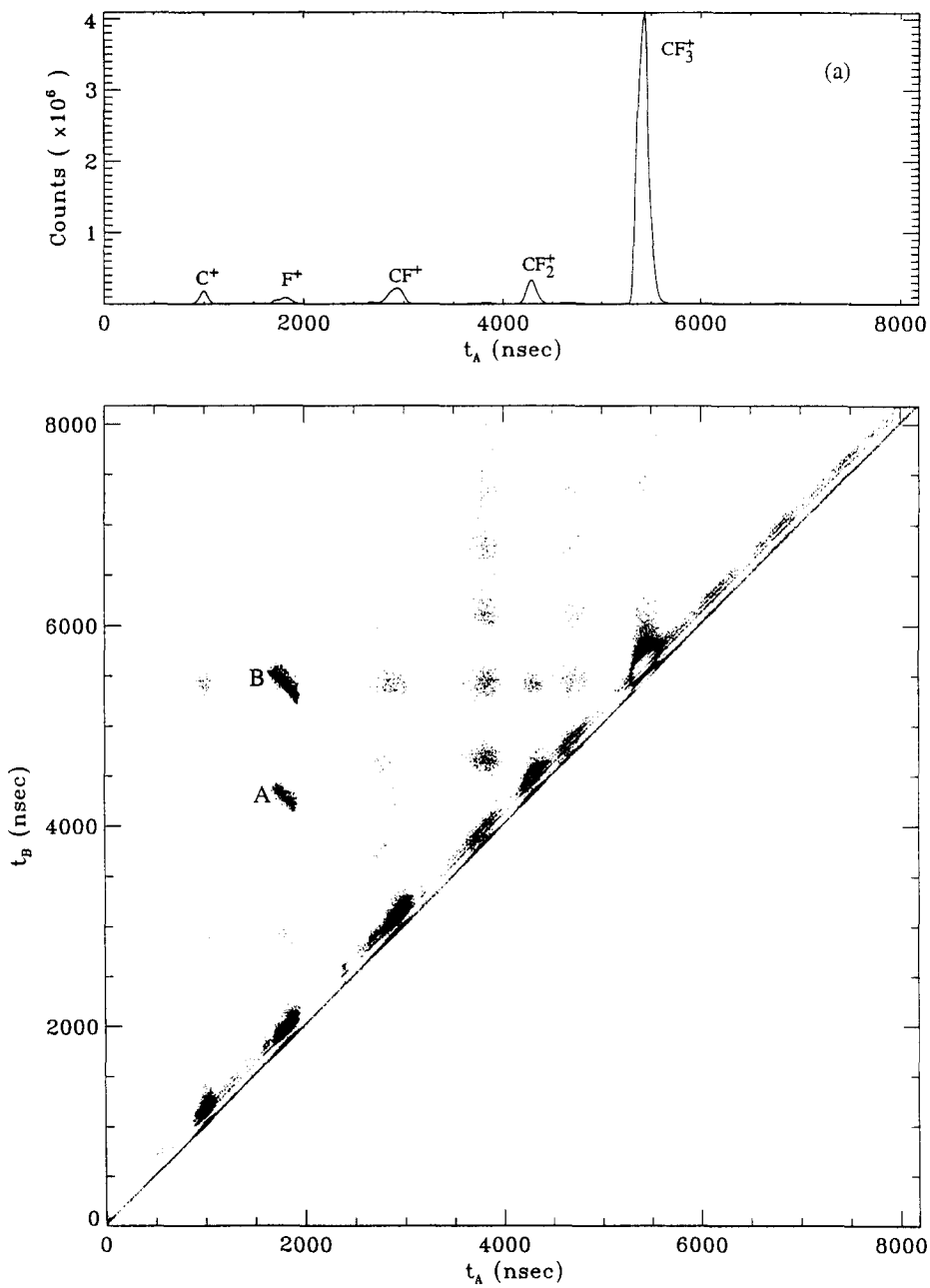

Fig. 1. (a) Positive ion–positive ion covariance map for CF_4 at an electron impact energy of 43.7 eV. The time-of-flight of the first (fast) ion is plotted on the horizontal axis and the second ion on the vertical axis. Feature A comes from the fragmentation reaction $CF_2^+ + F^+ + F$ and B comes from the reaction $CF_3^+ + F^+$. The TOF mass spectrum displayed at the top of the figure is the sum of all experiments in which only one positive ion was detected. The time scales of the two plots are identical and in nanoseconds.

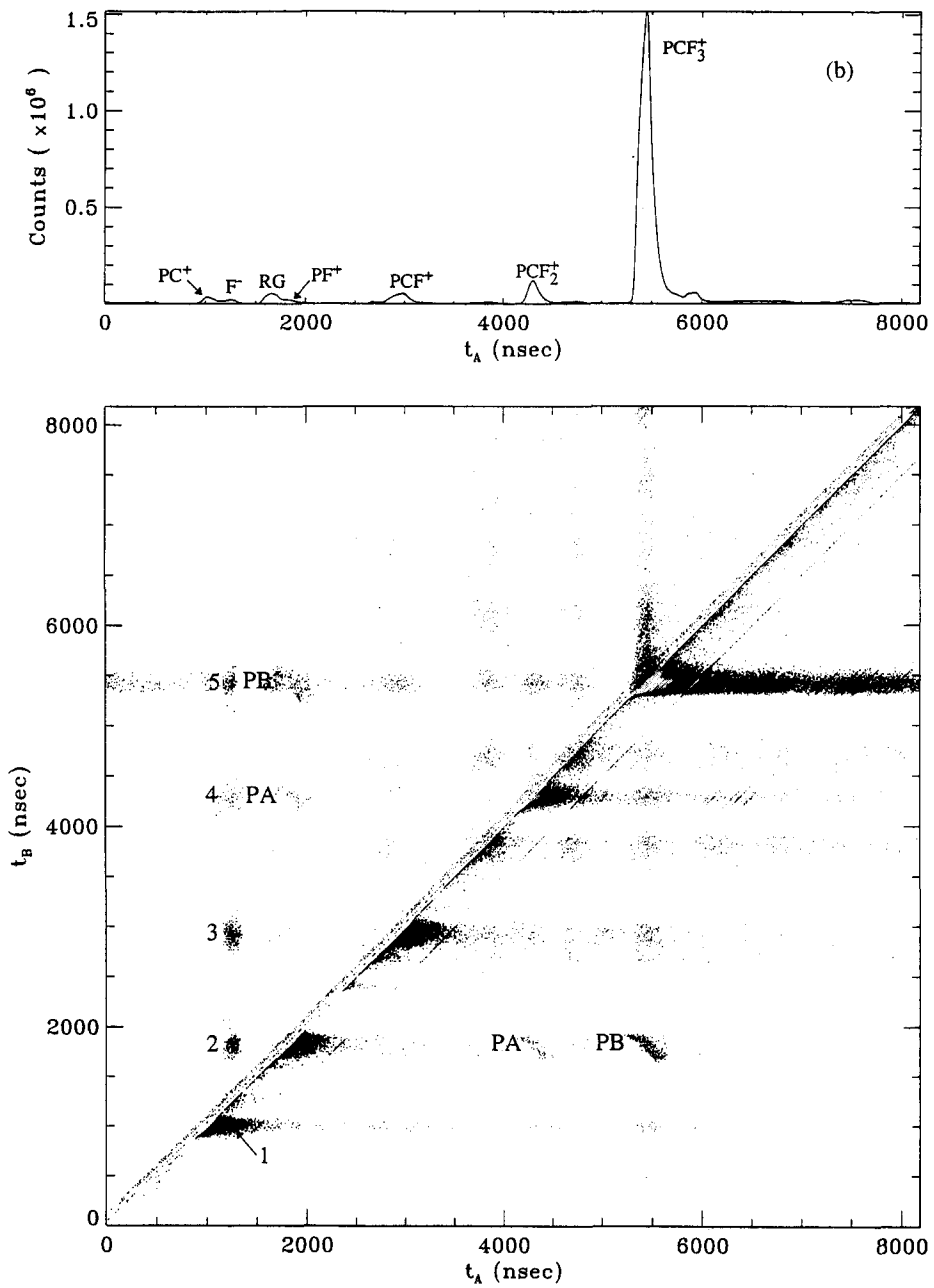

Fig. 1. Continued. (b) The positive ion–negative ion covariance map for CF_4 at an impact energy of 43.7 eV. The negative ion flight time is plotted on the horizontal axis. Features 1 through 5 are due to $C^+ + F^-$, $F^+ + F^-$, $CF^+ + F^-$, $CF_2^+ + F^-$, and $CF_3^+ + F^-$, respectively. The features PA and PB are pseudo negative ion–positive ion coincidences caused by back accelerated secondary electrons produced by positive ions hitting grids and detector. See text for a more complete description. The TOF mass spectrum displayed at the top of the figure is the sum of all experiments in which only one negative ion was detected. The peak labeled RG is due to secondary electrons from a grid in front of the 15 cm flight tube being struck by CF_3^+ ions. The time scales of the two plots are identical and in nanoseconds.

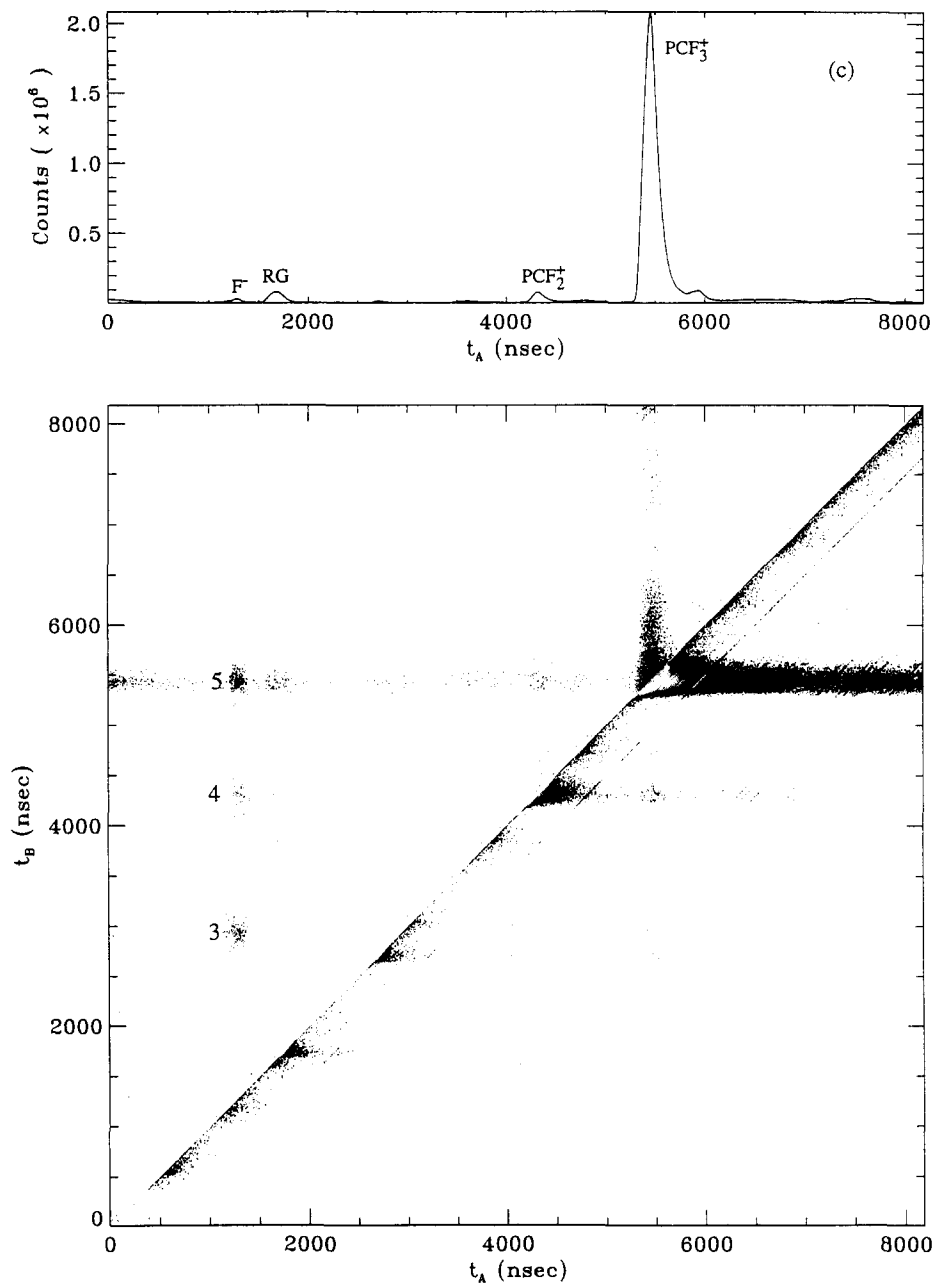

Fig. 1. Continued. (c) The positive ion–negative ion covariance map for CF_4 at an impact energy of 23.7 eV. See figure captions for (a) and (b) for further details. Note that only three of the five dissociation channels observed at 43.7 eV are open here. The TOF mass spectrum displayed at the top of the figure is the sum of all experiments in which only one negative ion was detected. The time scales of the two plots are identical and in nanoseconds.

displayed for an impact energy of 23.7 eV.

The covariance map, $C(t_-, t_+)$, where t_- is the flight time of the negative ion and t_+ is the flight time of the positive ion, is defined as

$$C(t_-, t_+) = [\langle I(t_-, t_+)\rangle - \langle I(t_-)\rangle \langle I'(t_+)\rangle / (T_a f)]/(T_a f), \quad (1)$$

where $\langle I(t_-, t_+)\rangle$ is the experimentally obtained coincidence map or cross correlation spectrum (all experiments in which one negative ion and one positive ion only are observed), $\langle I(t_-)\rangle$ is the experimental negative ion singles spectrum (all experiments in which only a single negative ion is observed), $\langle I'(t_+)\rangle$ is the experimental singles spectrum for positive ions, T_a is the total time in seconds that the experiment is acquiring data (total experimental run time corrected for dead time), and f is the frequency in units of s^{-1} of the electron gun pulser (number of experiments per second). Note that the product $T_a f$ is the total number of experiments, N, that were observed

The experimental details and references to other covariance mapping work can be found in Ref. [5]. Briefly, a pulsed electron beam of 5 ns fwhm (full width at half the maximum peak height) is incident on an effusive jet of the target gas (CF_4 in this case). After the electron pulse has left the scattering region (about 50 ns later) symmetrically placed extraction grids are pulsed to extract negative ions in one direction and positive ions in another (180° apart). The extraction field was 120 V/cm. The ions were further accelerated through a potential difference of 900 V and allowed to drift over a distance of 15 cm before a final acceleration through a potential difference of 3000 V 6 mm before crashing into the front surface of a multi plate micro channel plate detector. The second acceleration voltage (900 V), just before the two 15 cm drift tubes, was adjusted to a different value for negative ions than for positive ions, as explained later. In the case of the positive ion detector, the grid 6 mm in front of the detector was biased by both 300 V positive and negative, relative to the front surface potential of the detector (about 4000 V). The negative bias should suppress secondary electron loss with subsequent acceleration back to the negative ion detector, but it was discovered that the suppression was incomplete, probably due to secondary electron emission from the grids. All of the results reported here were obtained with a positive bias (positive ions accelerated in to the MCP). The impact energy was determined by observing fluorescent photons from a helium target gas beam in order to determine the absolute time scale to better than 1 ns. A shift of 3.7 eV to higher energy than that inferred from the accelerating potential in the electron gun was observed for each impact energy. The origin of this shift was not determined.

After the usual signal processing, the flight time of the first negative ion and the first two positive ions to arrive at their respective detectors were recorded by use of multi hit time to digital converters (TDC-LeCroy model 4208). The single event TOF (time-of-flight) spectrum for both positive and negative ions are accumulated as well as the cross correlation spectrum between positive and negative ions and between the first two positive ions [5]. Approximately 30000 experiments per second were performed with total data accumulation times of about 72 hours. The experiments were performed under single scattering conditions with total ion count rates of less than 100 counts per second.

From Figs. 1a–1c a number of observations can immediately be made. The polar dissociation map 1b contains strong features produced by correlations between positive ion signals and pseudo negative ion signals (features labeled PA and PB on the map). These occur because the positive ion count rates are very much larger than the negative ion count rates. Even our best attempts to prevent secondary electrons, produced at the front surface and grids of the positive ion detector, from reaching the negative ion detector are not 100% successful. Note that this effect causes the appearance of an apparent negative ion, delayed by the electron flight time (about 20 ns), for each positive ion detected. Because of this problem, we have offset the drift potentials, as mentioned earlier, so that electrons arriving at the negative ion detector for a particular positive ion mass will not interfere with an actual negative ion of the same mass. The magnitude of this shift can be observed in the negative ion singles spectrum shown at the top of Fig. 1b as the flight time difference between the F^- peak and the false peak labeled PF^+. The peak labeled RG in this spectrum is the result of secondary electrons produced by CF_3^+ ions striking a grid located in front of the 15 cm long

Table 1
Absolute cross sections in units of 10^{-24} m^2 (10^{-4} Å^2 or 10^{-2} Mb) for all observed polar dissociation channels in CF_4 from 18.7 to 43.7 eV

E (eV)	$CF_3^+ + F^-$	$CF_2^+ + F^-$	$CF^+ + F^-$	$F^+ + F^-$	$C^+ + F^-$	Total	Ref. [8] (2)
18.7	0.09					0.09	3
23.7	0.26	0.04	0.12			0.42	4
28.7	0.30	0.08	0.40	0.03	0.07	0.88	7
33.7	0.60	0.16	1.0	0.17	0.56	2.5	13
38.7	0.63	0.17	1.1	0.39	1.2	3.5	20
43.7	0.85	0.21	1.7	1.3	2.8	6.9	24

drift cell. At 43.7 eV impact energy there are only four clearly separated and one partially separated true positive ion–negative ion coincidence peaks (labeled 1 through 5 with 1 the partially separated feature). These correspond to $CF_3^+ + F^-(5)$, $CF_2^+ + F^-(4)$, $CF^+ + F^-(3)$, $F^+ + F^-(2)$, and $C^+ + F^-(1)$. The thermodynamic lower bounds (all fragments produced with zero translational energy) for the thresholds for these processes are 11.7, 17.4, 19.0, 22.4, and 26.3 eV, respectively. There appears to be a complete absence of positive ion correlations with negative ions other than F^-. This is in agreement with the photo excitation observations of Mitsuke et al. [3]. The pseudo features in the spectrum reproduce the positive ion–positive ion coincidence spectrum (compare PA and PB in Fig. 1b with the correlation features A and B in Fig. 1a) so that a direct comparison can be made with the negative ion–positive ion correlation peaks at the higher impact energies. It is immediately apparent that the length of the major axes of polar dissociation features are smaller than the major axes lengths of the positive ion–positive ion correlation features. This means that the fragment kinetic energies are smaller in the polar dissociation case. Several approximate theories are available for interpretation of the data [6,7], however we believe the uncertainties in the present data preclude further analysis except to note that most polar dissociation peaks show very little distortion, if any, from circular symmetry. This could be the result of the fact that the length of the major axes of the correlation features, which are proportional to the ion momenta and can be related to the separation energy, are about the same or less than the peak widths which are due to the finite volume of the initial ion cloud at the time of extraction. We estimate that the separation energy for the $CF_3^+ + F^-$ channel is less than 2.5 eV, which is in agreement with the photo excitation results [3]. The separation energies for the remaining channels appear to all be less than 5.5 eV. Estimates are based on the length of the long axis of the $CF_3^+ + F^+$ peak (feature B in Fig. 1a) which has a separation energy of about 10 eV. Since this work assumes that the only mechanism available for negative ion production is polar dissociation, there must be a connection between the sum of all events in the F^- mass channel and the F^- peak intensity in the negative ion singles spectrum. In fact, the latter intensity multiplied by the instrumental efficiency of the positive ion detector flight tube should be equal to the former. In order to check this we summed up the noise contribution as revealed by the covariance map and subtracted it from the singles spectrum. The remaining signal in the F^- channel of the negative ion singles spectrum divided by the positive ion instrumental efficiency agreed with the sum of events in the covariance F^- channel to within the statistical uncertainty. Hence, we believe that all negative ion production, at these energies, is due to polar dissociation processes.

In Table 1 estimates of the absolute values of the cross sections are given. The cross sections were determined by normalizing the intensity of the CF_3^+ peak in the singles spectrum to the absolute value of the partial ionization cross sections given in Ref. [8]. Because the positive and negative ion singles spectra, as well as the positive ion–positive ion and positive ion–negative ion covariance maps are recorded simultaneously, the placing of the CF_3^+ singles peak on an absolute scale automatically places all the other spectra on the same scale except that the covariance maps must be divided by the detector efficiency. The detector efficiency for positive ions was determined previously [9] while the negative ion detector efficiency was es-

timated from the manufacturers published grid transparency (90%/grid) and the difference between the relative detector efficiencies for positive and negative ions [10] (See Fig. 7 in this reference which shows what happens when no secondary electrons are collected, the positive ion case, and when the collection is maximized, the negative ion case.). We believe such an estimation process to be accurate to better than 15% since using the grid transparency and the detectors open area gives the positive ion detection efficiency to within 6%. Note that the sensitivity of our experiment on a typical 3 day data collection run is slightly better than 10^{-27} m^2 (10^{-7} Å^2 or 10^{-3} Mb) in regions of the covariance map that are not obstructed by noise.

The results reported in Ref. [2] appear to be too large although better agreement is obtained at higher impact energy ($\times 3$) than at lower ($\sim \times 30$). It should be pointed out however that the noise envelope of the F^- curve shown in Fig. 4 of Ref. [2] suggests that the values at 25 eV and below are uncertain by 100% or more. In addition, a weak magnetic field was employed to focus the electron beam in Ref. [2]. We would be concerned that at low electron impact energies such a field might cause electrons to orbit in such a way as to promote multiple electron collisions. Such a process would be more serious at lower impact energies. The magnetic fields in our apparatus were reduced to below 1 mG in the scattering region by means of extensive magnetic shielding. We also find no evidence at our sensitivity for the F_2^- channel reported by the authors of Ref. [2]. In Ref. [3] the authors reported that they carried out a very extensive search for negative ions, other than F^-, without success.

There are several puzzling aspects to the data in Table 1. The first is: why does the CF_2^+ product channel have such a small cross section? The second question is: why does the cross section, at the higher impact energies, increase as the number of product fragments increases? In addition, several of the channels seem to exhibit plateau regions followed by sharp increases as a function of increasing impact energy which may be indicative of higher excited states in the same mass channel. Further work will be necessary to answer these questions. In the photo excitation work reported in Ref. [3] all major features in the spectrum up to excitation energies of 31 eV were assigned to the $CF_3^+ + F^-$ break up channel. We cannot dispute this assignment, but can say that for some of the observed states that either the CF_3^+ ion must undergo further dissociation with a lifetime less than a few nanoseconds or else the other mass channels that we observe below 31 eV impact energy must be due to optically forbidden transitions.

Acknowledgement

The authors wish to acknowledge support of this work under NSF grant PHY 9214126.

References

[1] J.E. Ahnell and W.S. Koski, J. Chem. Phys. 62 (1975) 4474.
[2] I. Iga, M.V.V.S. Rao, S.K. Srivastava and J.C. Nogueira, Z. Physik D 24 (1992) 111.
[3] K. Mitsuke, S. Suzuki, T. Imamura and I. Koyano, J. Chem. Phys. 95 (1991) 2398.
[4] H. Yoshida and K. Mitsuke, J. Chem. Phys. 100 (1994) 8817.
[5] M.R. Bruce, L. Mi, C.R. Sporleder and R.A. Bonham, J. Phys. B 27 (1994) 5773.
[6] J.H.D. Eland, Mol. Phys. 61 (1987) 725.
[7] T. Baer, A.E. DePristo and J.J. Hermans, J. Chem. Phys. 76 (1982) 5917.
[8] R.A. Bonham, Japan. J. Appl. Phys. 33 (1994) 4157.
[9] M.R. Bruce and R.A. Bonham, J. Mol. Struct. 352/353 (1995) 235.
[10] C. Ma, C.R. Sporleder, and R.A. Bonham, Rev. Sci. Instrum. 62 (1991) 909 (see Fig. 7).